

Channel frequency optimization of spaceborne millimeter-wave radiometer for integrated water vapor retrieval in Arctic region

Haibo Zhao and Jungang Miao

Abstract—Water vapor information is very important to understanding global climate change, especially in the climatologically sensitive polar region. In 1998, Miao proposed a method to retrieve Integrated Water Vapor (IWV) content using SSM/T2 channels over the ice covered polar region. It has been proved to be effective in both Antarctic and partial Arctic region by subsequent studies. Unfortunately, with currently available millimeter radiometer channel combinations, the retrievable IWV content can not exceed 6kg/m^2 using Method of Miao. In this paper a new group of channel frequencies around 183GHz are established for a future AMSU-B-like radiometer, which is optimized for larger retrievable IWV range in Arctic region. Results show the retrievable IWV range has been expanded. The atmosphere profiles being used in the optimization process are *in situ* radiosonde data from IGRA, suggesting the optimized channel combination is not only workable in theory but also can be put into practice for IWV retrieval in Arctic region.

Keywords—channel frequency optimization, millimeter-wave radiometer, integrated water retrieval in Arctic region, passive microwave remote sensing

I. INTRODUCTION

Numeric modeling studies have shown that polar region is one of most sensitive region on Earth to global climate change [1]. And being the most abundant and the most radiatively important green house gas in the polar region [2],[3], water vapor does not only provide crucial information about climate change but also forms a feedback loop to it [4], so it is important to understand the quantity and distribution of atmospheric water vapor.

Spaceborne infrared and microwave radiometry have offered us powerful tools understand water vapor information in the troposphere [5]-[7]. In the year of 1998 Miao proposed a IWV retrieval algorithm above ice covered polar region based on spaceborne millimeter-wave radiometry [8], and has been proved to be effective for IWV retrieval in both Antarctic and partial Arctic region [9], [10].

Manuscript submitted on February 3, 2009. This work is supported by the National Natural Science Foundation of China under grants #40476061 and #40525015.

Haibo Zhao is with Electronics Engineering and Information Department of Beihang University, China.(phone: 86-010-82317214; Email: zhaohaibo0813 @126.com)

Jungang Miao is with Electronics Engineering and Information Department of Beihang University, China. (Email: jmiaobremen @buaa.edu.cn)

Unfortunately, however, this method is bound to some limitations, one of them is that, with currently available radiometer channel combinations (SSM/T2 and AMSU-B, etc.), the retrievable IWV content can not exceed 6kg/m^2 [8], which is generally satisfied within the Antarctic Region. But when trying to use Method of Miao to the whole Arctic Region, one problem appears: in the Arctic Region, the IWV content is usually higher than that of Antarctic Region (See Fig.1); retrieval of IWV can only be done at certain limited areas and time (See Fig.2). The most important reason for this limitation is the selection of SSM/T2 and AMSU-B channel frequencies ($89, 150, 183 \pm 7, \pm 3, \pm 1$ GHz, etc.), which is primarily targeting for water vapor profile retrieval in the low and mid-latitude areas, and may not be optimized for IWV retrieval in polar regions.

It is known that, the farther a channel is located from 183GHz absorption peak, the less sensitive and more tolerant (can see through the atmosphere, not just sensitive to the water vapor in the upper troposphere) it is to water vapor. So in order to expand the retrievable IWV range with Method of Miao, it is necessary to find possible double-sideband channel combinations located farther to 183GHz than available SSM/T2, AMSU-B channels (the farthest being $183 \pm 7\text{GHz}$). In this paper, up to ± 37 GHz around 183GHz are considered (See Fig.3) and clear sky condition is assumed through out the simulation.

II. RADIATIVE TRANSFER MODEL AND DATASET

A. Radiative Transfer Model

The radiative transfer model used in this paper is VDISORT [11], the version we used is last modified by the author in April 2000. The program is written in Fortran 90, and compiled with Compaq Visual FORTRAN 6.6 under Windows platform. The millimeter-wave absorption module in the program is adopted from Rosenkranz [12].

B. Dataset

The polar region radiosonde profile data in this work are adopted from IGRA (Integrated Global Radiosonde Archive).

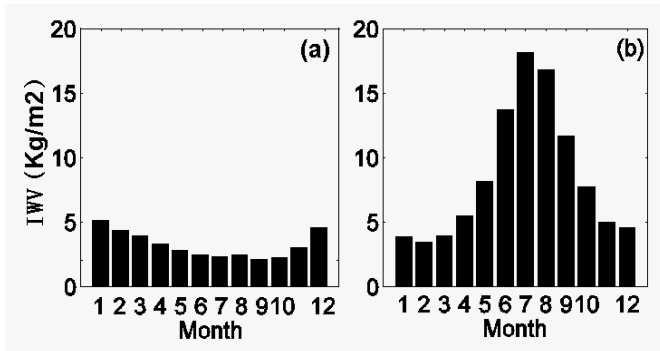


Fig.1 Mean IWV monthly distribution calculated from IGRA for (a) Antarctic Region and (b) Arctic Region

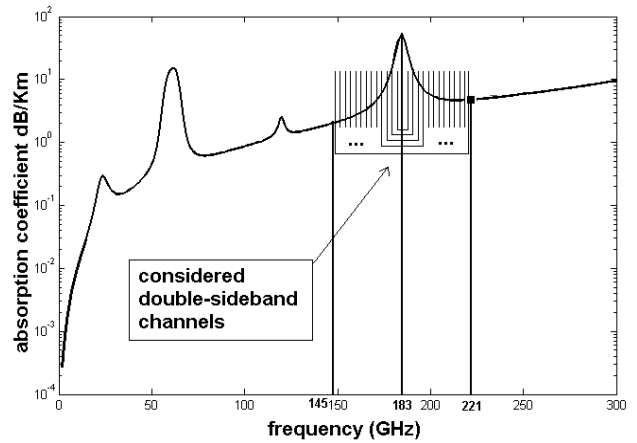


Fig. 3 Considered double-sideband channels

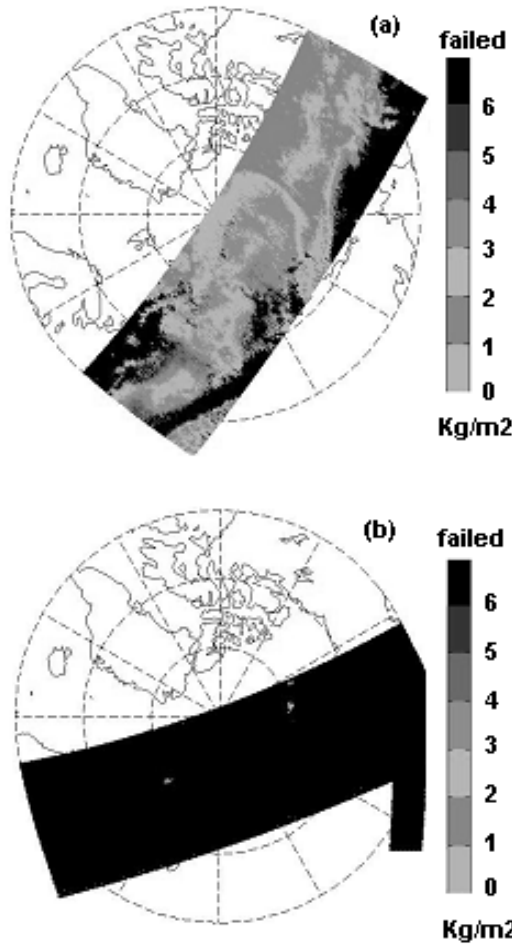


Fig.2 IWV retrieval in the Arctic region using AMSU-B measurements, (a) February, (b) July, black area means IWV can not be retrieved with AMSU-B channels

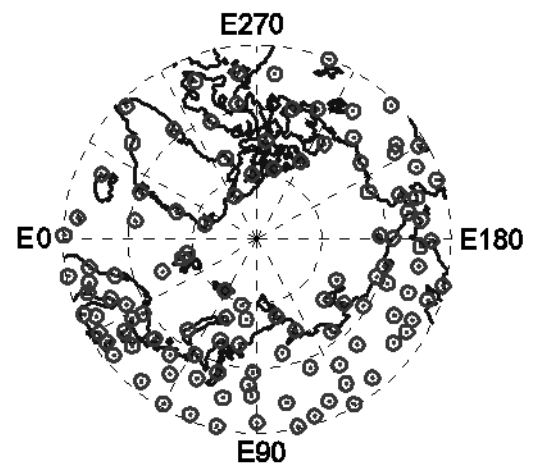


Fig.4 Arctic weather stations used in IGRA

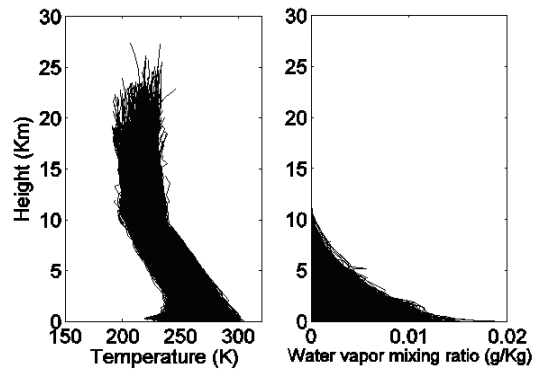


Fig. 5 Truncated profiles for Arctic Region (10412 profiles)

IGRA is new radiosonde dataset from the National Climate Data Center (NCDC). IGRA contains quality-assured data from 11 different sources. Rigorous procedures are employed to ensure proper station identification, eliminate duplicate levels within soundings, and select one sounding for every station, date, and time [13].

VDISORT requires the number of levels for input atmosphere profiles to be constant, and in the top-down order. So we select those profiles from IGRA whose number of levels ≥ 30 and ≤ 45 , sort the levels in the right order and truncate the top ones, leaving a constant 25 levels per profile. Finally we select 10412 profiles within the Arctic Circle (Latitude ≥ 66.5) (See Fig.4) in the year of 2007. The error

introduced by the level truncation process is expected to be small, because the water vapor mixing ratio of top levels being truncated is 0. (See Fig.5)

III. METHODOLOGY

A. Ice Surface Emissivity Modeling

The Method of Miao is based on the assumption that emissivity is constant in the range of 150-200GHz. This assumption turns out not to be a good one according to airborne measurements, and error introduced in the retrieved IWV could be substantial in many cases [9]. So the inconstancy of ice emissivity at each channel frequency point has to be taken into consideration for channel optimization. In this paper we adopt the emissivity field measurement data of six types of ice from SEPOR-POLEX campaign [10]. The emissivity for six kinds of ice at frequency 157GHz and 183GHz are listed below: (See Table 1). And according to the work of Selbach, the overall correlation of the six types of ice between this two frequency points is 0.9884[10].

Table 1. Emissivity statistical data at 157GHz and 183GHz

Ice Type	157GHz		183GHz	
	Mean	Std	Mean	Std
Open Water	0.712	0.005	0.732	0.007
Nilas	0.922	0.015	0.919	0.016
Pancake	0.866	0.023	0.873	0.022
First-year Flat	0.733	0.036	0.763	0.032
First-year Ridged	0.724	0.053	0.752	0.045
Multi-year	0.709	0.039	0.740	0.033

Because the emissivity statistical data is only available at three frequency points (89GHz, 157GHz and 183GHz) from SEPOR-POLEX campaign, the emissivity at $183.31 \pm 1, \pm 2, \dots, \pm 38$ GHz are obtained by linear interpolation and extrapolation satisfying the correlation coefficient of 0.9884 between 157GHz and 183GHz. This process is detailed below:

(1) Generate six sets of 8286 Gaussian distributed random numbers satisfying the mean and standard deviation of six kinds of ice at 183GHz respectively to simulate the emissivity for six kinds of ice surfaces used in the radiative transfer model, being noted as $Em(183)$.

(2) Assume the emissivity satisfying linear relationship in the range of 183-38GHz and 183+38GHz, i.e.

$$Em(f) = Em(183) + A \times (183 - f)$$

f is in the range of 183-38GHz and 183+38GHz, A is a constant coefficient for each type of ice. Therefore we have:

$$Em(157) = Em(183) + A \times (183 - 157)$$

according to the mean value of each ice type at 157GHz and 183GHz, A can be derived. Now we can get 77 sets of

numbers for each ice type ($Em(145), \dots, Em(221)$), representing the emissivity at 77 frequency points, the mean value of each set satisfies the above emissivity mean value relationship. Due to the linear form adopted, the correlation coefficient of emissivity at any two frequency point is 1.

(3) Introduce 8286 Gaussian distributed random numbers with mean value 0, standard deviation σ noted as $G(+1)$, add $G(+1)$ into $Em(183+1)$, introduce another set of Gaussian distributed random numbers with the same mean value 0 and standard deviation σ , add it to $G(+1)$ to form $G(+2)$ then add $G(+2)$ into $Em(183+2)$ and so on till we get $Em(183+38)$. $Em(183-1) \dots Em(183-38)$ are obtained in the same way. With this process, the correlation coefficient is bigger at nearer frequency points, which is a physically reasonable assumption.

(4) Calculate the correlation coefficient of $Em(157)$ and $Em(183)$, if it is smaller than 0.9884, reduce σ and if it is bigger, increase σ and repeat step (3), till we find a proper σ to satisfy the field measurement data whose correlation coefficient between 157GHz and 183GHz is 0.9884 (See Fig. 4, 5)

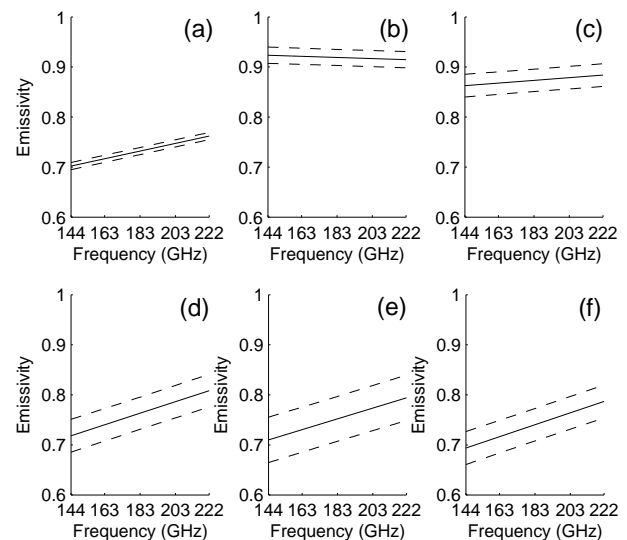


Fig.4 Generated ice emissivity for 6 kinds of ice surfaces at frequency 144, 145, ..., 222 GHz, solid lines represent mean emissivity, dash lines represent their rms at each frequency point, for (a) Open Water (b) Nilas (c) Pancake (d) First-year Flat (e) First-year Ridged (f) Multiyear

B. Regression Coefficients

As stated in the introduction, if we want to expand the retrievable IWV range using Method of Miao, possible

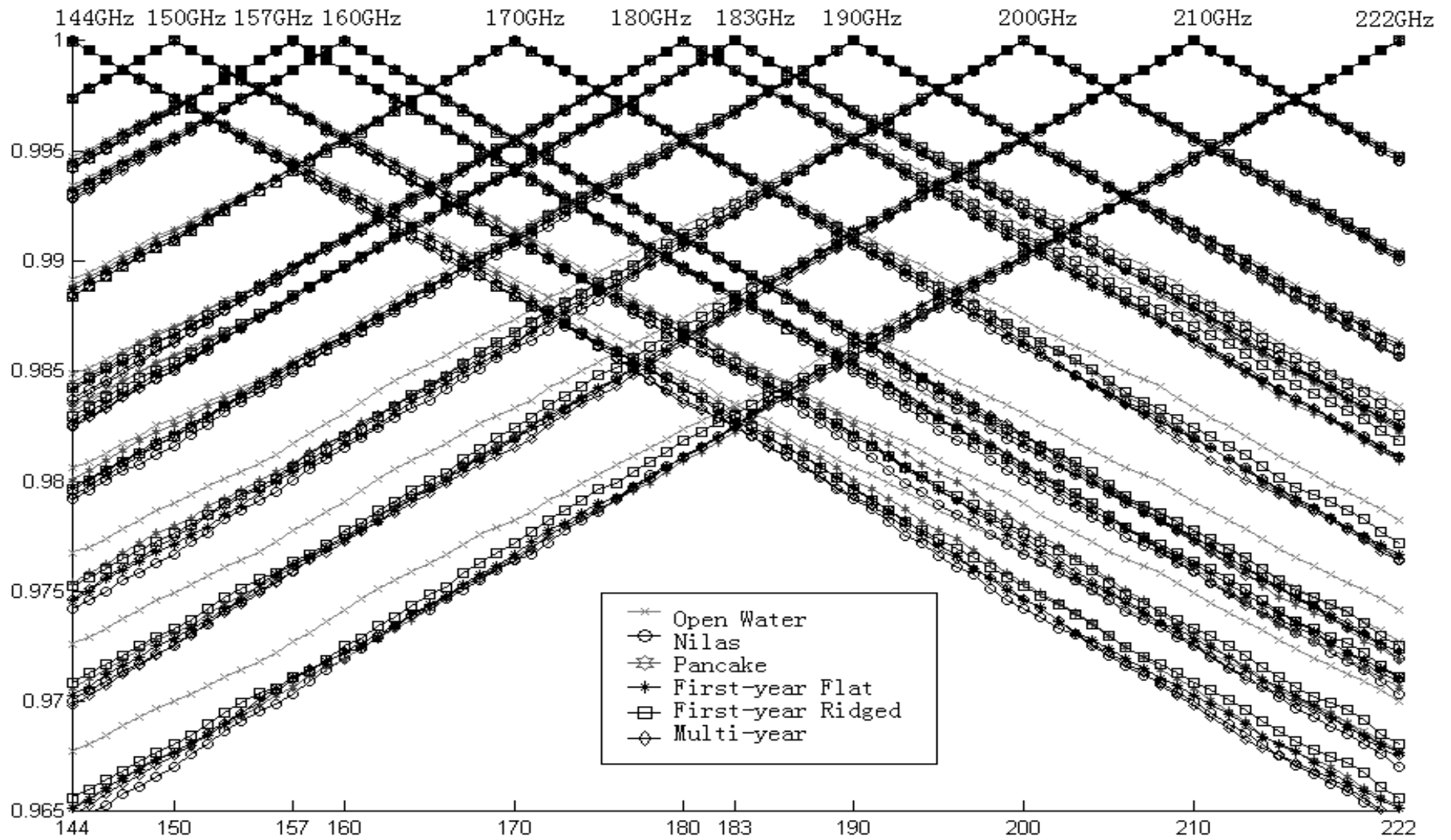


Fig.5 Correlation coefficients for generated surface emissivity at frequency points 144, 150, 157, 160,170, 180, 183, 190, 200, 210, 222 GHz relative to other frequency points in the range of 144~222 GHz

channels should be located farther to 183GHz absorption peak than available water vapor profiling channels. Here, up to ± 37 GHz unpolarized channels are considered ($183.31 \pm 1, \pm 2, \dots, \pm 37$ GHz). According to the work of Miao, sideband is located symmetrically about 183GHz to cancel surface emissivity difference [8], it is also possible because we have assumed that the emissivity satisfy linear relationship in the frequency range of 183-37GHz \sim 183+37GHz as stated in section III.A.

The brightness temperatures (T_b) of corresponding channels with different surface emissivities ($\epsilon_r = 0.6, 0.7, 0.8, 0.9, 1.0$) and scan angles (scan angle = 1.5, 45 degree) are calculated using the VDISORT radiative transfer model. The brightness temperature for each sideband is obtained by a three frequency points (f_0-1 GHz, f_0, f_0+1 GHz, f_0 is the center frequency of a sideband) average to simulate a 2GHz bandwidth, and the T_b for a double-sideband channel is obtained by the average of two sidebands.

Later a subtraction between two channels from the 37 double-sideband channels is performed. There are 666 such subtractions ($C_{37}^2 = 666$). From the 2-channel combinations a select-2 combination is performed again to achieve the preliminary 4-channel combinations ($C_{666}^2 = 221,445$). One thing to be noted is with the two-step procedure, 3-channel combinations originally used by Miao (See Fig. 6) are completely included in the more generalized 4-channel combinations.

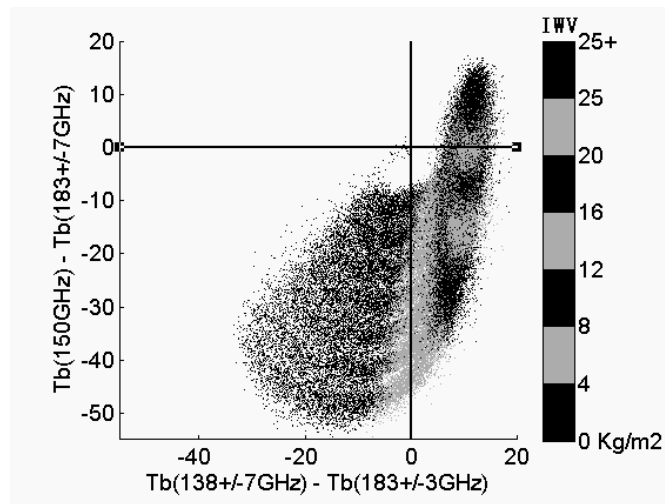


Fig. 6 Original channel combination (3-channel combination) of SSM/T2 used by Miao

We calculate the brightness temperature for half of the 8268 selected profiles (1 to 4134, regression group) with surface emissivity set to 0.6, 0.7, 0.8, 0.9 and 1.0 respectively and according to the Method of Miao [8], the regression coefficients (C_0, C_1, X_0, Y_0) corresponding to each 4-channel combination can be obtained.

C. Retrieved IWV for Each 4-channel Combinations

The brightness temperatures of the other half of 8286 profiles (4135 to 8286, test group) are calculated with modeled ice emissivity in section III.A, and 3 frequency points average is done in the same way to simulate 2GHz bandwidth.

Using the regression coefficients derived in 3.2, we can now obtain the retrieved IWV. Just before that, a 0.5K noise is introduced into each double sideband channel. The noise is simulated by a set of Gaussian distributed random numbers with mean value 0.0, and standard deviation 0.5.

With some computer efforts, the retrieved IWVs for each 4-channel combination above 6 kinds of ice surfaces are calculated; the rms and bias between the actual IWV (calculated from radiosonde) and retrieved IWV are readily obtained. Because we introduced 0.5K noise, the final rms and bias are obtained by the average of 100 recalculations, results show 100 recalculation average can assure significant number of 1 decimal point (See Fig. 7).

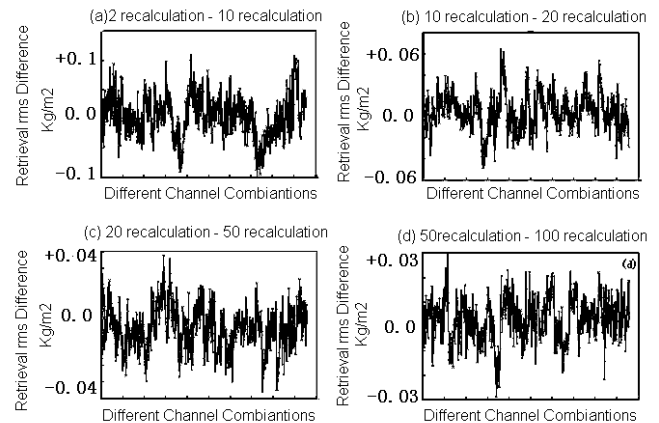


Fig7. Retrieval rms difference between recalculations

We confine the rms of the retrieved IWV within a certain value, leaving 1% (about 2200) 4-channel combinations for each ice type with smallest rms, and they are our preliminary choices (See Fig. 8, 9).

The IWV retrieval rms for the six types of ice surfaces can be roughly classified into 3 groups: (1) Open Water, (2) First-year Flat, First-year Ridged, and Multiyear, (3) Nilas and Pancake. The IWV uncertainty for class (1) is about 12.3%, for class (2) is about 14.7%, and for class (3) is 28.6%. This classification is because lower and more uniform surface emissivity can offer a more desirable background for IWV retrieval with spaceborne radiometer.

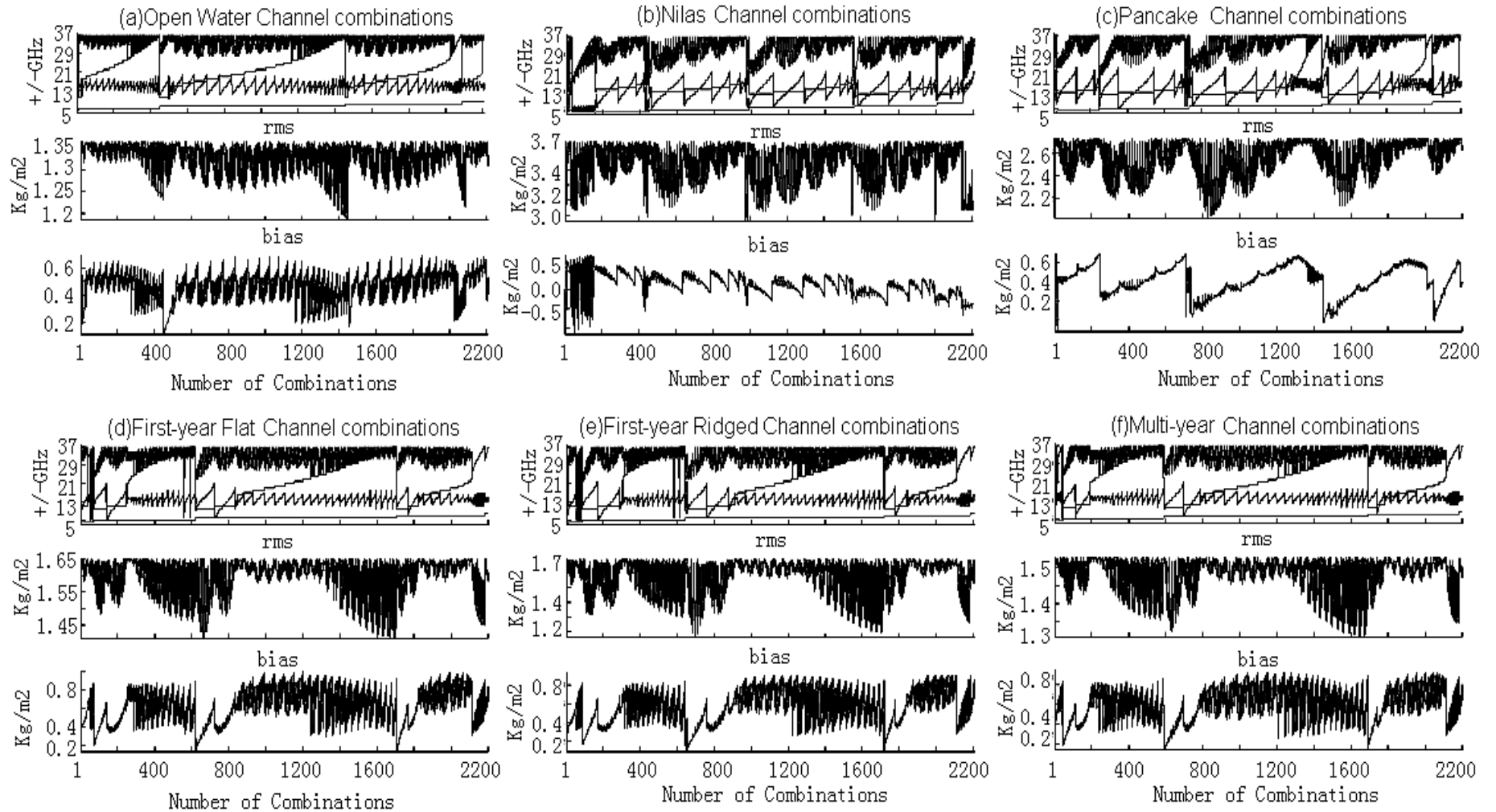


Fig.8 preliminary 4-Channel combinations above six types of ice surfaces, scan angle = 1.5 degree

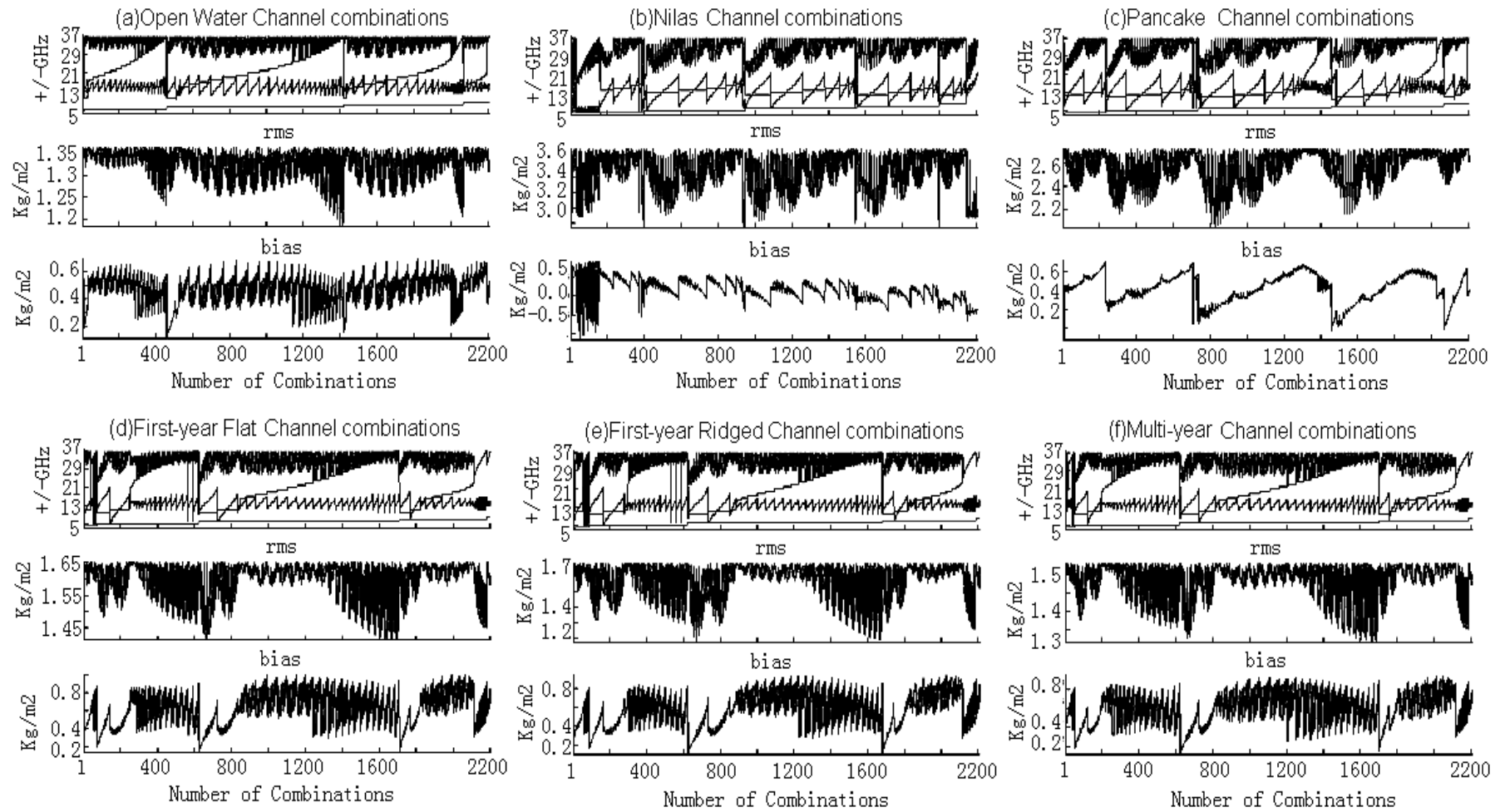


Fig.9 preliminary 4-Channel combinations above six types of ice surfaces, scan angle = 45 degree

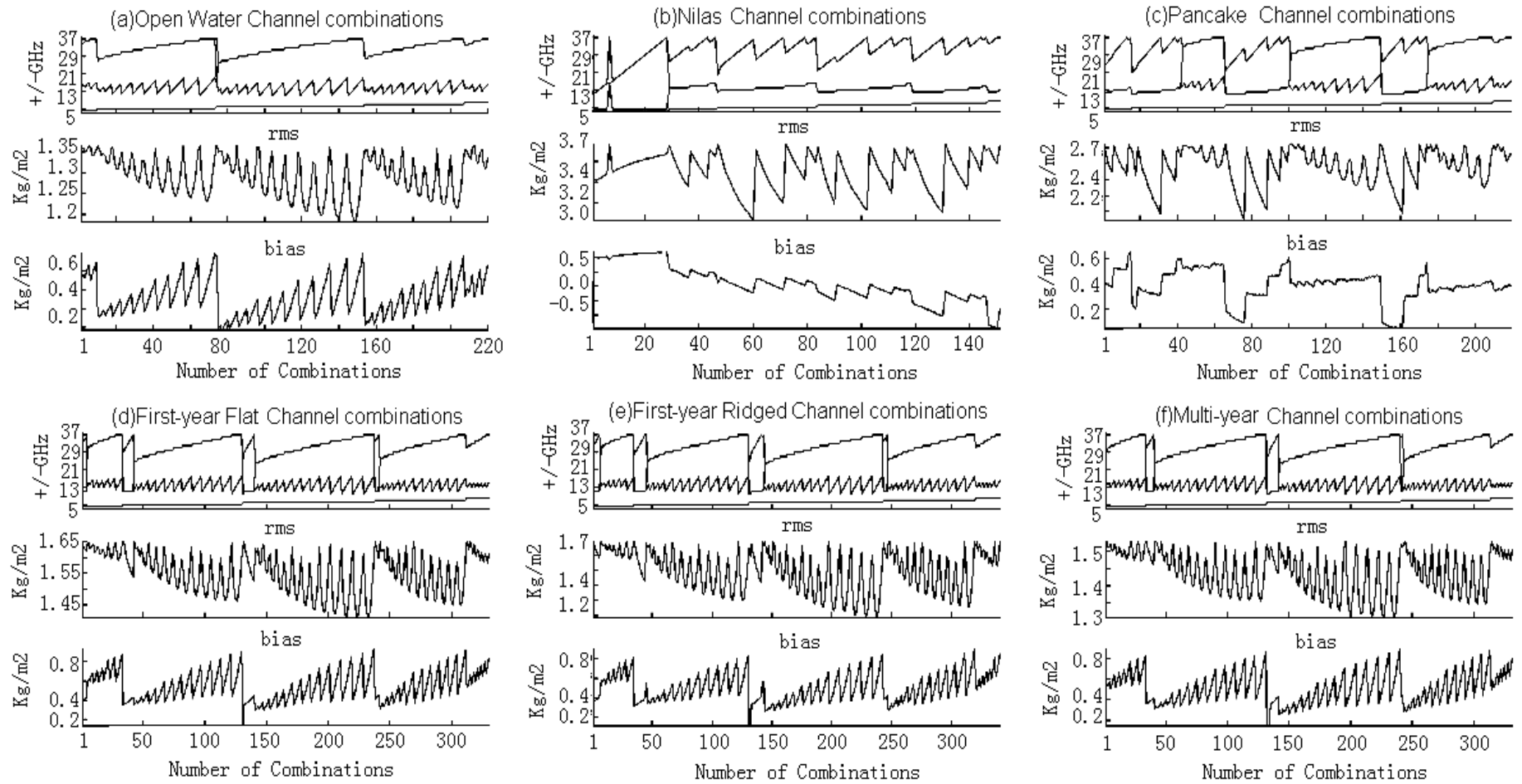


Fig.10 the included 3-Channel combinations above six types of ice surfaces, scan angle = 1.5 degree

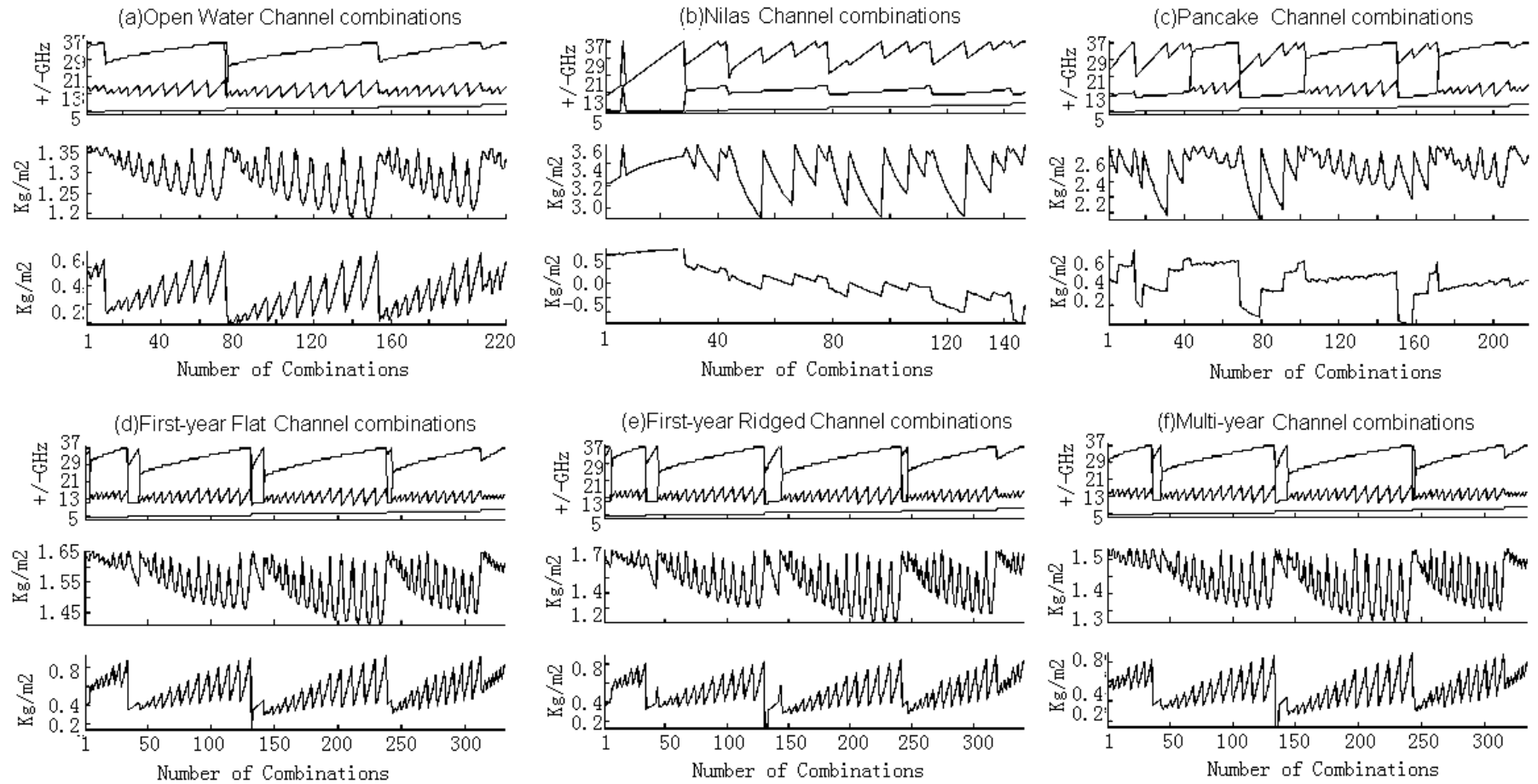


Fig.11 the included 3-Channel combinations above six types of ice surfaces, scan angle = 45 degree

D. Final 3-channel Combination

Considering the economics of space-borne platform, further choices are focused on the 3-channel combinations included in the 4-channel combinations. Figure 10, 11 are the 3-channel combinations for each ice surfaces with scan angle=1.5, 45 degree respectively.

We try to find a common 3-channel combination to all of the six ice surfaces, unfortunately, there is none. There is, however, a 3-channel combination: $Tb(183 \pm 37GHz) - Tb(183 \pm 17GHz) / Tb(183 \pm 37GHz) - Tb(183 \pm 7GHz)$ (See Fig. 12), common to five of the ice types except Nilas, and it is consist of frequencies with great compatibility with currently available radiometers:

Channels or passbands already used by other radiometers: $183+37 GHz = 220GHz$ (MIR) [14]-[16], $183 \pm 7GHz$ (AMSU) [17];

Channels or passbands close to other radiometers or development under way: $183-37GHz = 146GHz \approx 150GHz$ (AMSU, "window spectrum" can be replaced by 150GHz) [17], $183 \pm 17GHz$ (GOMAS).

And as a matter of fact, none of the 3-channel combinations for Nilas is common to the other five ice types, because Nilas is a distinguished ice type, whose emissivity is exceptionally high and variant (See Fig. 4). Further calculation shows that the special 3-channel combination mentioned above can be also be used above Nilas, only the IWV retrieval rms is poor (See Fig. 15, 16).

IV. DISCUSSIONS

The IWV retrieval performance of 2200 preliminary 4-channel combinations is quite comparable (Fig. 8, 9), thus we propose the final optimized channel combination which has best compatibility with currently available radiometers. And considering the economics of spaceborne platform, the included 3-channel combinations are our priority choices.

The selection of optimized channel combinations is rather robust, i.e. for each channel, all frequencies in certain ranges are applicable to form workable combinations, take open water surface, scan angle=1.5° case for example, the possible channel combinations and ranges for each channel are shown in Fig. 13 and Fig. 14.

We can see from Fig. 15 and Fig. 16, there are considerable system biases for each type of ice surfaces. It is because the atmospheric absorption characteristic at the wing of 183GHz is not strictly symmetric, and here we used symmetric passbands about 183GHz, therefore, the influence of surface emissivity can not be fully compensated, it is one problem that we need to consider in the future.

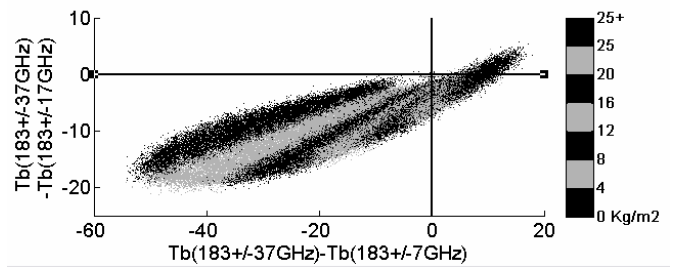


Fig.12 The optimized 3-channel combination: $(183 \pm 37GHz - 183 \pm 17GHz) / (183 \pm 37GHz - 183 \pm 7GHz)$

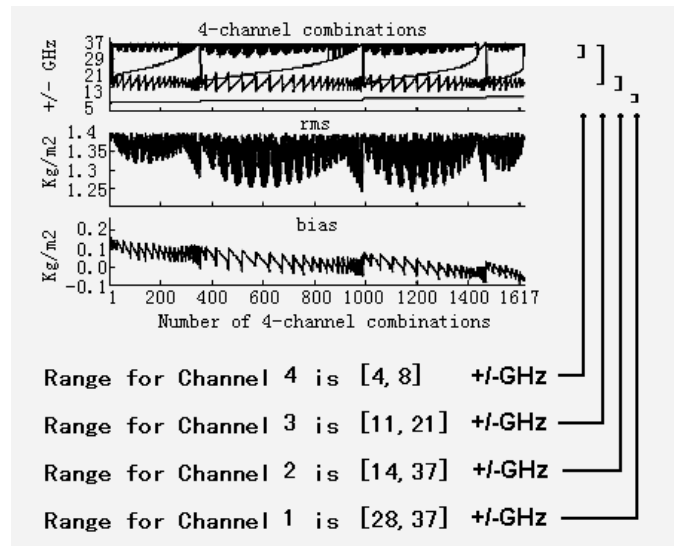


Fig. 13 4-channel combinations and frequency ranges for each channel, open water surface, scan angle=1.5°

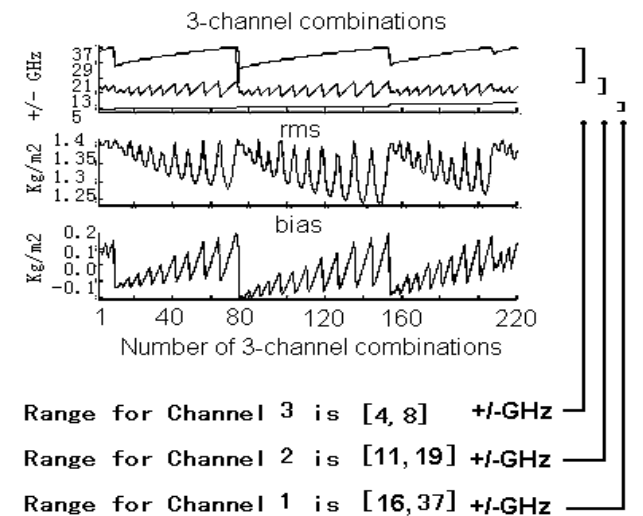


Fig. 14 3-channel combinations and frequency ranges for each channel, open water surface, scan angle=1.5°

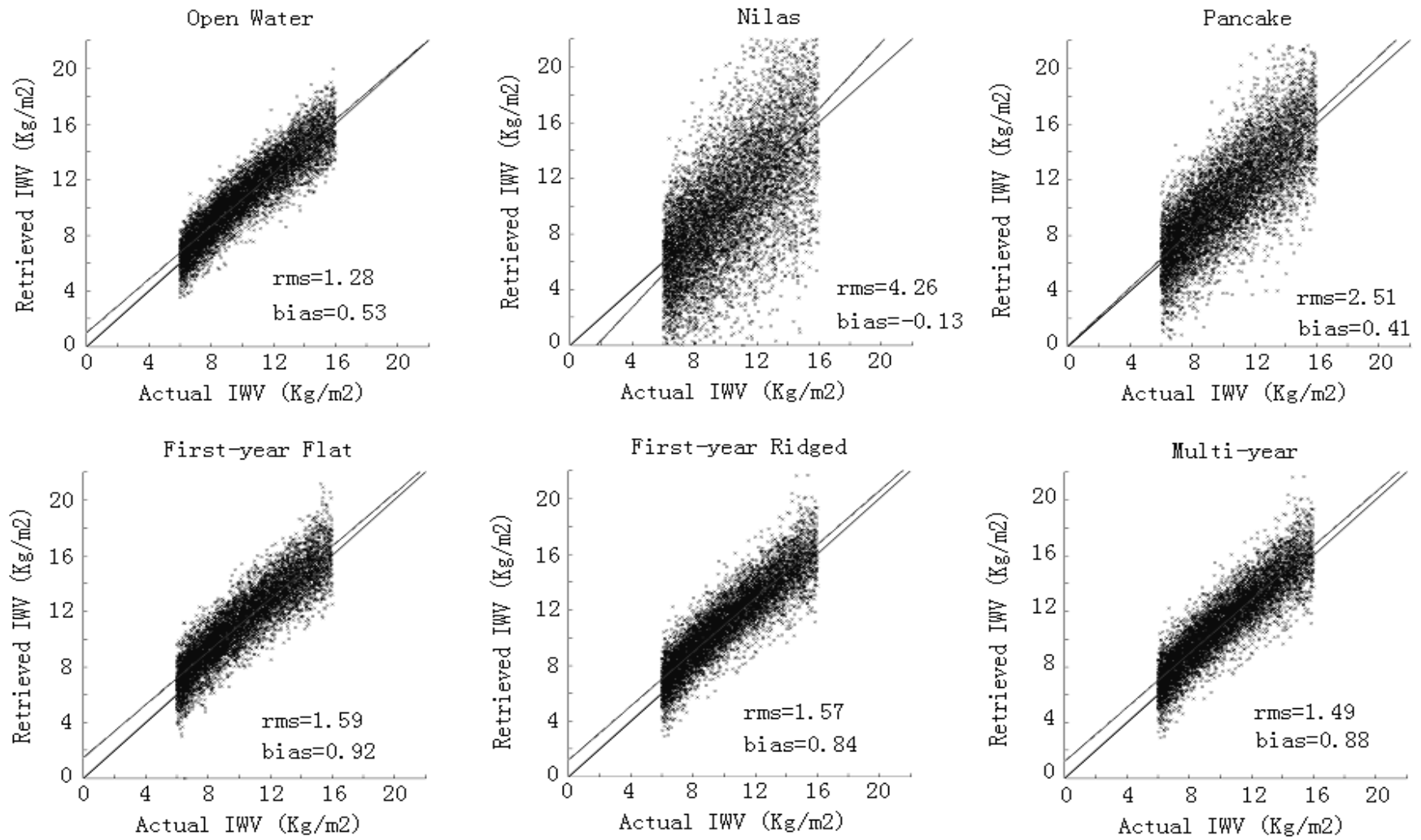


Fig.15 IWW retrieval performance for channel combination $(183 \pm 37\text{GHz} - 183 \pm 17\text{GHz}) / (183 \pm 37\text{GHz} - 183 \pm 7\text{GHz})$ above six kinds of ice surfaces, angle=1.5 degree

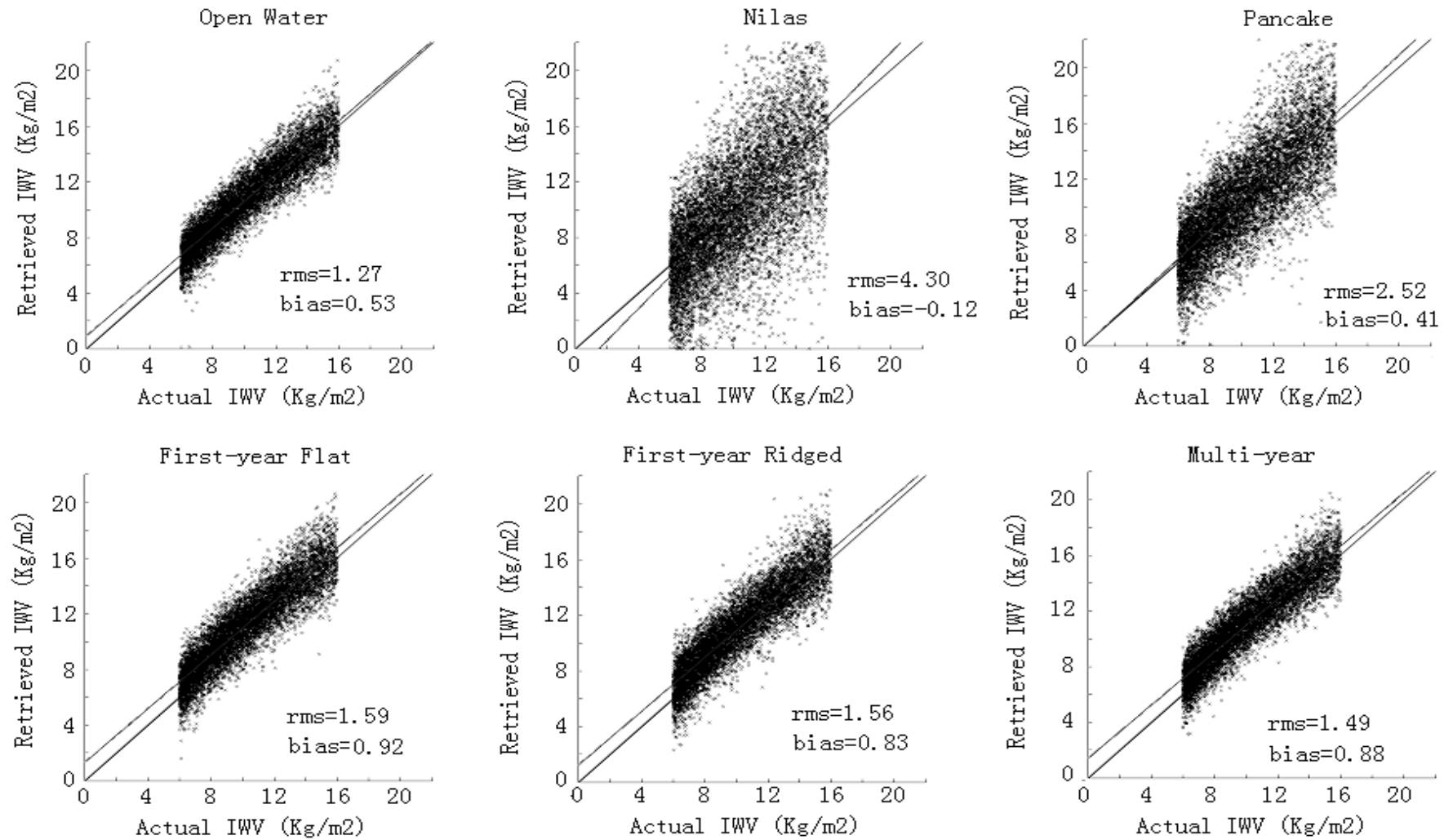


Fig.16 I WV retrieval performance for channel combination $(183 \pm 37\text{GHz} - 183 \pm 17\text{GHz}) / (183 \pm 37\text{GHz} - 183 \pm 7\text{GHz})$ above six kinds of ice surfaces, angle=45 degree

V. CONCLUSION AND FUTURE WORK

In this paper, the optimized channel combinations for IWV retrieval in the polar regions with Method of Miao are proposed. Optimization is mainly targeting for the expansion of retrievable IWV range. Results show the upper retrievable IWV range expands from 6Kg/m² to 16Kg/m². And considering the compatibility with currently available radiometer channels, an optimized 3-channel combination: Tb(183 ± 37GHz) – Tb(183 ± 17GHz) / Tb(183 ± 37GHz) – Tb(183 ± 7GHz) is the best trade-off choice.

Calculation uses in situ Arctic radiosonde data, the results show the newly proposed channel combination is applicable for both scan angles (1.5, 45 degree) above six types of ice surfaces. It suggests the optimized channel combinations are suitable for spaceborne platform and can be put into practice for IWV retrieval in polar regions.

The surface modeling in this paper is based on linear interpolation and extrapolation using statistical value from SEPOR-POLEX campaign, which is the closest knowledge we have on ice emissivity around 183GHz. More realistic modeling will be adopted when new theory or field experiment result is available.

All channels being simulated are unpolarized, with symmetric passbands about 183GHz, polarization and asymmetric passbands will be considered in the future.

The general usefulness (water vapor profiling in a global scale, performance under cloudy conditions, offering other weather products, etc.) of the newly proposed channels still needs to be studied, and it's possible that we have to find a compromise between other usages and the performance of IWV retrieval in polar regions.

VI. APPENDIX

The regression coefficients (C0, C1), focal point (X0, Y0) (K) [8], retrieval error rms, bias (Kg/m²) for channel combination Tb(183 ± 37GHz) – Tb(183 ± 17GHz) / Tb(183 ± 37GHz) – Tb(183 ± 7GHz) above six types of ice surfaces for scan angle 1.5 and 45 are listed below:

C0	C1	X0	Y0	rms	bias
Scan Angle=1.5					
25	16.2	8.89	2.05	1.28	0.53
25	16.2	8.89	2.06	4.26	-0.13
25	16.2	8.89	2.05	2.51	0.41
25	16.2	8.89	2.05	1.59	0.92
25	16.2	8.89	2.06	1.57	0.84
25	16.2	8.89	2.06	1.49	0.88
Scan Angle=45					
25	16.2	8.89	2.06	1.27	0.53
25	16.2	8.89	2.06	4.3	-0.12
25	16.2	8.89	2.06	2.52	0.41

25	16.2	8.89	2.06	1.59	0.92
25	16.2	8.89	2.06	1.56	0.83
25	16.2	8.89	2.06	1.49	0.88

References:

- [1] R. G. Barry, M. C. Serreze, J. A. Maslanik, and R.H. Preller, "The Arctic Sea Ice-Climate System: Observations and Modeling", *Review of Geophysics*, vol. 31, NO.4, 1993, pp.397-422
- [2] C. Melsheimer, and Georg Heygster, "Improved retrieval of total water vapor over polar region from AMSU-B microwave radiometer data", *IEEE Transaction on Geoscience and Remote Sensing*, vol.46, NO.8, 2008, pp2307-2322
- [3] D. V. Vladutescu, Y. Wu, and L. Charles, "Water vapor mixing ratio used in lidar calibration technique", *Proceeding of the 2nd WSEAS International Conference on Remote Sensing*, Spain, 2006, pp68-76.
- [4] J.-P. Blanchet, E. Girard, "Water vapor-temperature feedback in the formation of continental Arctic air: its implication for climate", *The Science of the Total Environment* vol.160/161, 1995, pp. 793-802
- [5] X. Liu, M. Mlynczak, D. Jonhson, D. Kratz, H. Latvakosk, and G. Bingham, "Atmospheric Remote Sensing using FIRST (Far Infrared Spectroscopy of the Troposphere instrument)", *2005 WSEAS Int. Conf. on REMOTE SENSING*, Italy, 2005, pp5-10.
- [6] D. Staelin, "Passive Remote Sensing at Microwave Wavelengths", *Proceeding of the IEEE*, vol. 57, NO.4, 1969, pp427-439.
- [7] K. Klaes, "The EPS/Metop System as a contribution to Operational Meteorology and Earth System Monitoring", *2005 WSEAS Int. Conf. on REMOTE SENSING*, Italy, 2005, pp43-48.
- [8] J. Miao, K. Kunzi, and G. Heygster, "Atmospheric water vapor over Antarctica derived from Special Sensor Microwave/Temperature 2 data". *Journal of Geophysical Research*, vol.106, NO.D10, 2001, pp.187-203.
- [9] J. R. Wang, P. E. Racette, and M. E. Triesky, "Retrieval of precipitable water by the millimeter-wave imaging radiometer in the Arctic region during FIRE-ACE", *IEEE Transactions Geoscience and Remote Sensing*, vol. 39 NO.3 2001, pp 695-605.
- [10] N. Selbach, "Determination of column water vapor and surface emissivity of sea ice at 89GHz, 157GHz and 183GHz in the Arctic winter", Ph.D. Thesis, Dept. Physics, Univ. Bremen, Bremen, Germany, 2003, pp191
- [11] F. M. Schulz, K. Stamnes, F. Weng, "VDISORT: An Improved Generalized Discrete Ordinate Method for polarized (Vector) Radiative Transfer", *J. Quant. Radiat. Transfer* vol.61, NO1, 1999, pp.105-122

[12] P. Rosenkranz, "Absorption of microwaves by atmospheric gases", *Atmospheric Remote Sensing by Microwave Radiometry*, ch. 2. New York: Wiley, M. A. Janssen, Ed. 1993

[13] I. Durre, R. S. Vose, and D. B. Wuertz, "Overview of the Integrated Global Radiosonde Archive", *Journal of Climate*: vol. 19, NO. 1, 2006, pp. 53-68

[14] J.R. Wang, and W. Manning, "Retrievals of Low Integrated Water Vapor Using MIR and SSM/T-2 Measurements", *IEEE Transactions on Geoscience and Remote Sensing*, vol.41 NO 3, 2003, pp. 630-639

[15] J.R. Wang, P. Racette, M.E. Triesky, and W. Manning, "Retrievals of Column Water Vapor Using Millimeter-wave Radiometric Measurements", *IEEE Transactions on Geoscience and Remote Sensing*, vol. 40, NO.6, 2002, pp. 1220-1229

[16] P. Racette et al., "Measurement of Low Amounts of Precipitable Water Vapor Using Ground-Based Millimeterwave Radiometry", *Journal of Atmospheric and Ocean Technology*, vol.22, 2005, pp. 317-337

[17] F. Weng: "Operational AMSU Products and Their Applications", *Proc. Optical Remote Sensing of the Atmosphere and Clouds III*, Hangzhou, China, SPIE, 2003, pp.36-44